A R C H I V E O F M E C H A N I C A L E N G I N E E R I N G

Volume 66 2019 Number 1

DOI: 10.24425/ame.2019.126373

Key words: skull, shape, imaging precision, spiral computed tomography, reverse engineering

Andrzej Ryniewicz[1,2], Wojciech Ryniewicz[3], Stanisław Wyrąbek[1], Łukasz Bojko[4]

Evaluation of skull bone structures in CT imaging

At the current stage of diagnostics and therapy, it is necessary to perform a geometric evaluation of facial skull bone structures basing upon virtually reconstructed objects or replicated objects with reverse engineering. The objective hereof is an analysis of imaging precision for cranial bone structures basing upon spiral tomography and in relation to the reference model with the use of laser scanning. Evaluated was the precision of skull reconstruction in 3D printing, and it was compared with the real object, topography model and reference model. The performed investigations allowed identifying the CT imaging accuracy for cranial bone structures the development of and 3D models as well as replicating its shape in printed models. The execution of the project permits one to determine the uncertainty of components in the following procedures: CT imaging, development of numerical models and 3D printing of objects, which allows one to determine the complex uncertainty in medical applications.

1. Introduction

At the current stage of diagnostics and therapy, there is a need to carry out a geometric evaluation of facial skull bone structures basing upon virtually reconstructed or replicated objects by using reverse engineering [1]. The shape and geometry of the facial skull depend, to a great extent, on individual features. Extensive individual variety can be observed for people of different race, age and sex [2].

✉ Andrzej Ryniewicz, e-mail: andrzej@ryniewicz.pl

[1]Cracow University of Technology, Faculty of Mechanical Engineering, Poland. Email: st.wyrobek@gmail.com

[2]State University of Applied Science, Nowy Sącz, Poland.

[3]Jagiellonian University Medical College, Faculty of Medicine, Dental Institute, Department of Dental Prosthodontics, Cracow, Poland. Email: wojciech@ryniewicz.pl

[4]AGH University of Science and Technology, Faculty of Mechanical Engineering and Robotics, Department of Machine Design and Technology, Cracow, Poland. Email: lbojko@agh.edu.pl

It may also be influenced by diseases and traumas. Many factors have an impact on the precision of imaging while using computer tomography (CT) [3–5]. One of them is spatial resolution, which determines the ability to differentiate between the details of an image [6–8]. The greater the spatial resolution, the greater the precision of the imaging of examined structures. Contrast resolution, which determines the ability to differentiate between small objects and provides information on the correct value of radiation absorption in Hounsfield units, is also important [9, 10]. It plays a significant role in the environment in which the radiation absorption values for neighbouring tissues are similar. Another factor is time resolution. The sooner the measurement is made, the more effectively movement artefacts can be eliminated [8, 11, 12].

The project is aimed at analyzing the precision of imagining for the shapes of skull bone structures reconstructed on the basis of spiral tomography as compared with the reference model prepared by using laser scanning. Moreover, the precision of skull imaging in a 3D print was evaluated [13–15]. The print was made on the basis of the CT numerical model and compared with the reference model, too.

2. Material and method

The research material was a skull from the collection of the Museum of Anatomy of the Jagiellonian University Medical College. Object imaging was performed on a Somatom Emotion tomograph made by Siemens using the spiral technology at the Computer Tomography Laboratory of the MSWiA Hospital in Cracow. The numerical model of this skull was generated after the DICOM data were imported to the 3D Slicer 4.6.2 programme. The obtained model was smoothed out with Autodesk Meshmixer programme and basing thereupon, a model based on the net of triangles was developed (Fig. 1) [16]. The Invivo 5.3 program

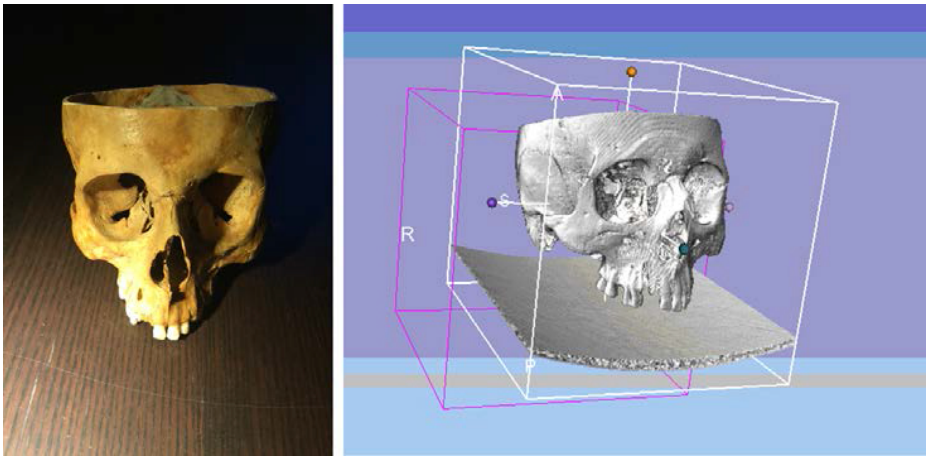

Fig. 1. A skull and its model reconstructed basing upon CT imaging

by Anatomage, Inc. was used to analyze tomographic images. The separation of hard tissues from air was carried out because of bone density in Hounsfield units. Hounsfield unit, is an approximate value of the voxel calculated by "Rescale Slope" (the incline angle of re-scaling) and "Rescale Intercept" (intersection point with the axis of the re-scaling angle) in DICOM information.

The reference model was the skull model prepared by using laser scanning (Fig. 2).

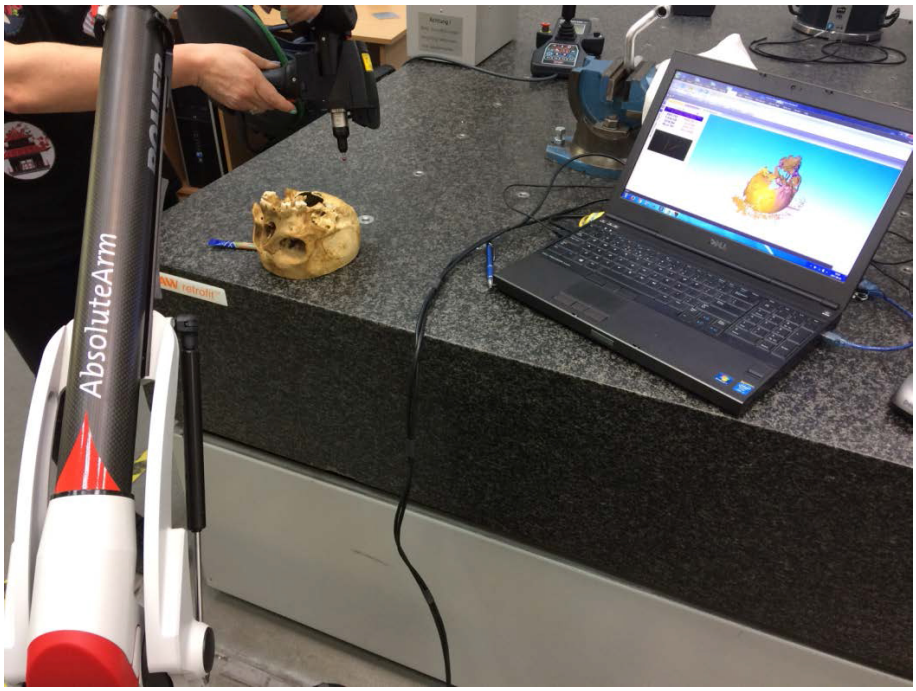

Fig. 2. A procedure for making a skull reference model

The measurements were carried out by using the Romer AbsoluteArm RA – 7320 SI scanner with a laser head at the Laboratory of Coordinate Metrology at Cracow University of Technology. The reference model, as assumed in the considerations, determined by means of a measuring arm with a test laser head confirmed the acceptance of the obtained results as a reference model. The evaluation of imaging precision for the skull reconstructed on the basis of CT was performed in the GOM Inspekt 2017 programme using the best fit method and compared to the reference model [17].

The next stage was to print the skull on the basis of the CT model by using the Rep Rap i3 printer, FDM model (Fig. 3) [18, 19]. The printed object was scanned on a laser scanner and then a numerical model was developed [13, 14]. The imaging precision of the printed model was evaluated by using the abovementioned method for both the CT model and the reference model.

Fig. 3. A printed skull model

To properly carry out the experiment, measurement strategy was adopted [20, 21]:

- location and orientation of the object of measurement and pattern in the same plane and working space,
- the same strategy for collecting measurement points, i.e., the same amount (> 20) and the method for collecting measurement points,
- the same type and kind of the measuring head,
- identical environmental conditions.

Medical metrology aims to determine the standard deviation depending on the individual, complex shape of objects and on the errors that are associated with the idea of measurement and the method of creating an object in reverse engineering. The selected parameters were evaluated and their standard deviations were determined.

3. Results and discussion

The following models were compared in order to evaluate the precision of bone structure imaging:

- the CT model and the reference model,
- the printed model and the CT model,
- the printed model and the reference model.

As a result of the comparison of the CT model and the reference model of the skull, the average deviations of the mapping in the range of ± 0.35 mm were ascertained (Fig. 4). While analyzing the map of deviations for this configuration,

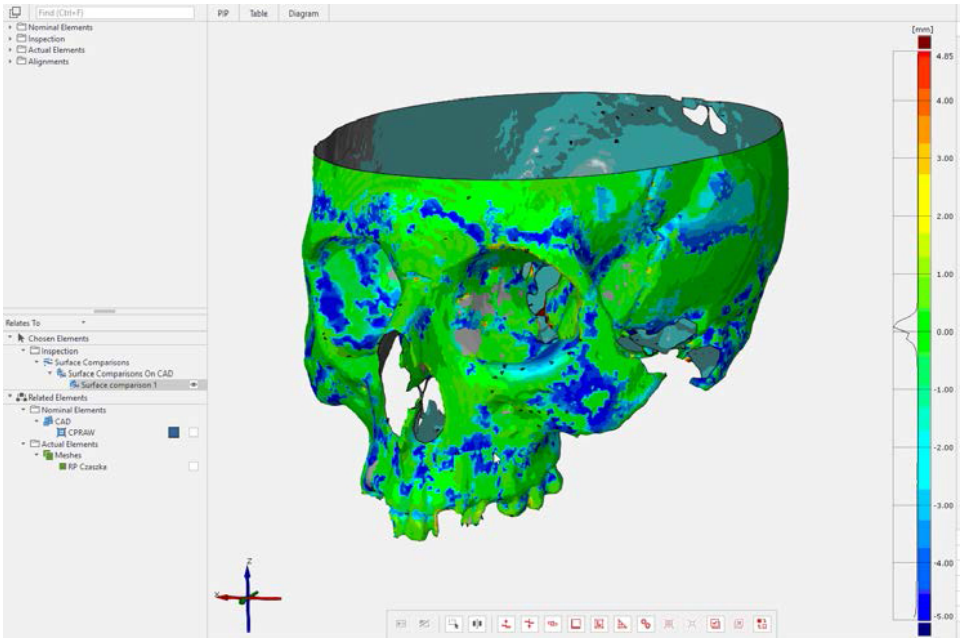

Fig. 4. A map of deviations for the comparison between the CT model and the reference model of the skull

it may be stated that the maximum deviation values were in the area of the greatest irregularities of the skull shape and depended on its position in relation to the plane determined by the laser beam inside the gantry. The effect of the object shape and its location within the measuring area upon the CT imaging precision was confirmed in the investigations into ball models [10, 17, 22]. A map of imaging precision for a ceramic ball surface, subject to CT investigations and reconstructed in 3D Reshaper program – when compared to the ideal CAD model (Fig. 5 and 6) – indicates an increase in the errors of ball surface imaging with a decrease of phantom circles in the successive scanning planes. The greatest errors with values of −0.021 mm were found in two areas referred to as tomography poles. Such a distribution of CT imaging errors for the reference ball model implied a deformation consisting in a surface flattening in the polar zones [25].

After CT investigations into spatial models and an analysis of measurement results one can state that the strongest effect upon the shape imaging precision was due to the thickness of the layer under imaging, resolution and the field of vision [24–26]. Imaging precision errors, especially on free surfaces, depend on: the shape of the surface under imaging and its inclination to the scanning plane, homogeneity of radiation and geometry of formation of scanning planes as well as on the positioning and selected mobile assemblies. Observed is an effect of understated diameters of ball models, which results from the anisotropic deformations in three planes. Spiral tomography introduces an imaging error for

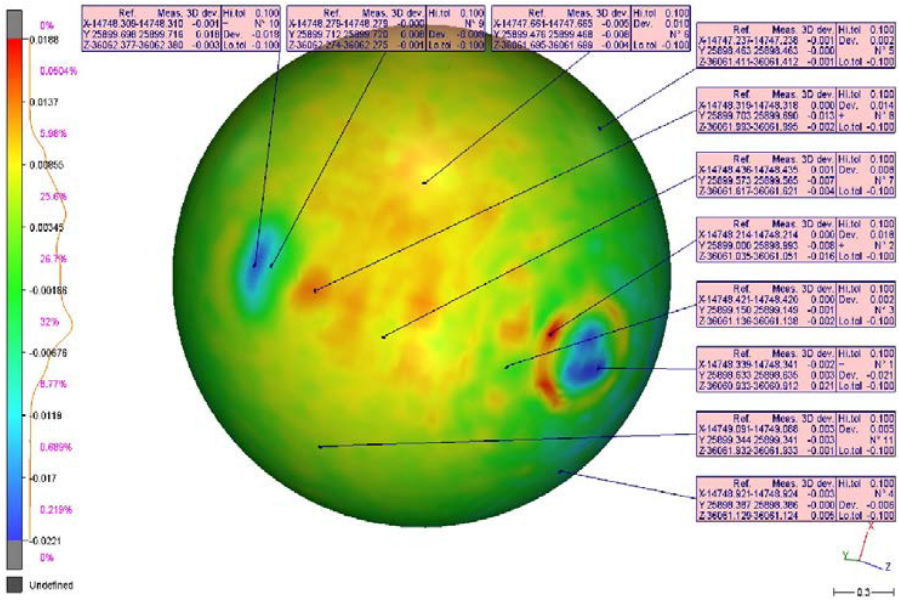

Fig. 5. A map of imaging precision for the ceramic ball surface, subject to CT investigations and reconstructed in 3D Reshaper, compared to an ideal CAD

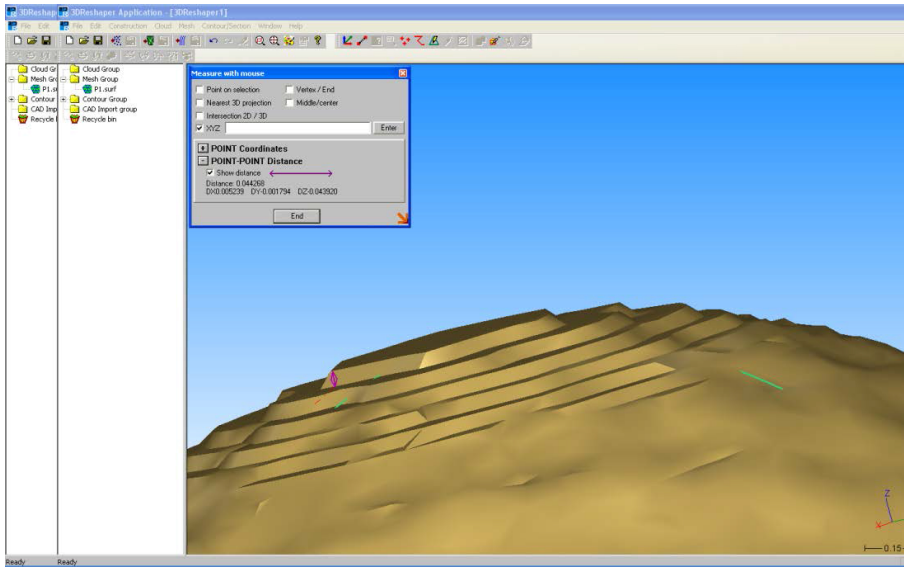

Fig. 6. Tomography pole in the CT model of ceramic reference ball

free shapes, which arises from the scanning method, thickness of measurement layer, radiation properties and kinematic parameters of tomography assemblies, as well as the software used for the analysis [27, 28].

The deviations between the printed model and the CT model fell within the range of ±1.5 mm, but the deviations greater than 0.75 mm were confirmed for just 2% of the tested area (Fig. 7). The deviations between the printed model and the reference model achieved the values within the range of +2.29 mm and −2.56 mm, but the end-of-the-spectrum values were confirmed only for 1.2% of the entire surface (Fig. 8) [29].

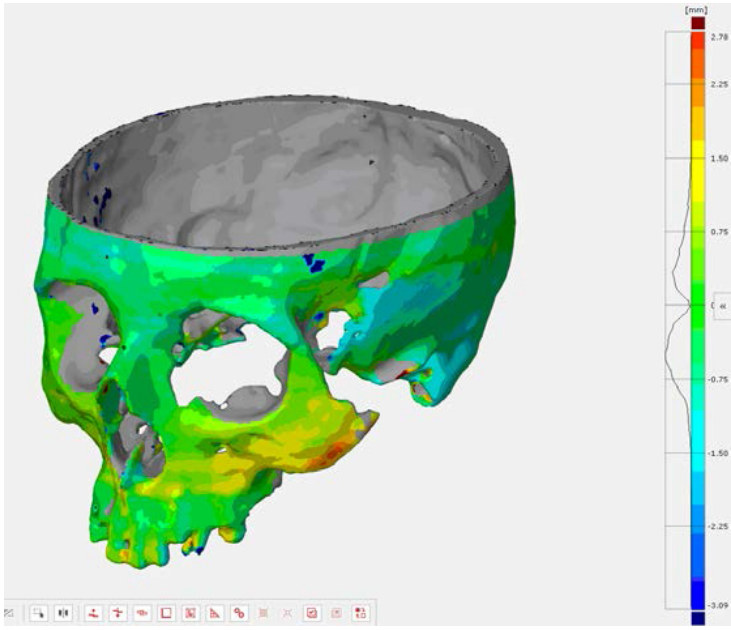

Fig. 7. A map of deviations for the comparison between the printed model and the tomography model

They occurred primarily within the area of the zygomatic bone and teeth – i.e., in the places where corrections were introduced to the CT model in order to adjust it to the requirements of the printer control system [12, 30].

The imaging precision for the dimensions in the printed model was checked for the selected geometric parameters with the application of a retrofitted ZKM measuring microscope with incremental rules and a Renishaw controller and Quindos software.

Measurement points were determined upon the object of investigations, on its numerical model and the printed model (Fig. 9). The measurement results are gathered in tables (Table 1) and on the graph illustrating the relation occurring between the measurement results for a real object and the type of its model (Fig. 10).

The obtained measurement results imply that the CT imaging-based numerical models can reconstruct the real object with an error in the interval from 1.5% to 4.5%; prevailing are negative errors. In the printed model ascertained were errors of shape imaging errors ranging from 2% to 9.5%. The error distribution in this

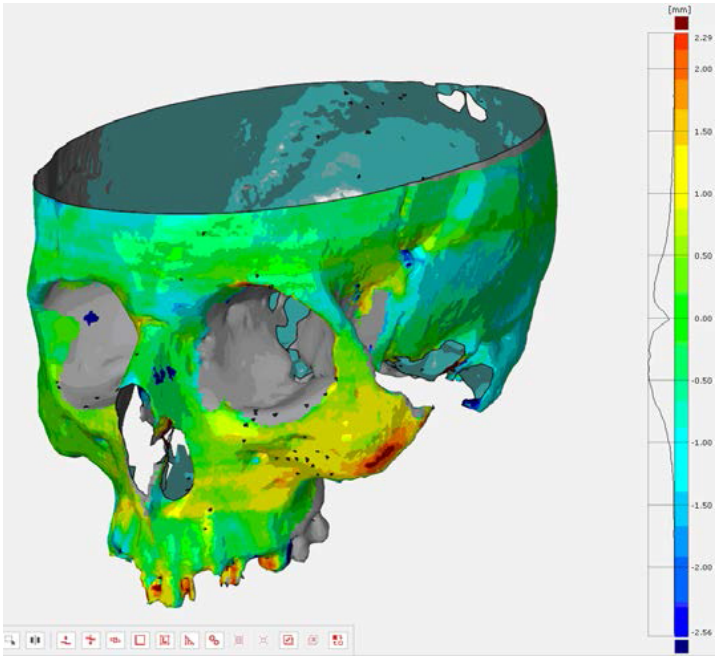

Fig. 8. A map of deviations for the comparison between the printed model in correlation with the reference model

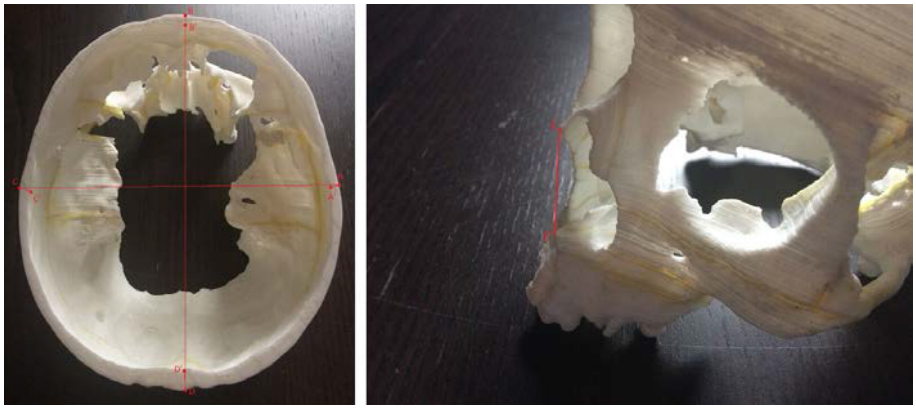

Fig. 9. Exemplary geometric parameters marked on the printed model

model depends upon the object surface complexity, geometric irregularity, and especially, upon curvature radii. Measurements of selected geometric parameters proved that in the printed model appear artefacts which cause changes in sizes, viz., increasing or decreasing their real values. The nature of such changes depend upon the assumed measurement strategy and research procedures. At the same time, the error distribution for the imaging of geometric parameters related to the thickness

Table 1.
Measurement results for selected geometric parameters of the real object, tomographic model and printed model

Measured parameter	No. measurement	The real model [mm]	Tomographic model [mm]	Printed model [mm]
AA′	1	3,22	3,08	3,88
	2	3.06	3.22	3.90
	3	2.87	2.85	3.75
	4	3.30	2.82	3.78
	5	3.11	3.01	3.69
	Average value	3.11	2.99	3.81
	Standard deviation	0.15	0.15	0.09
BB′	1	3.51	3.42	2.94
	2	3.50	3.35	2.95
	3	3.32	3.29	3.05
	4	3.58	3.55	3.27
	5	3.50	3.56	3.21
	Average value	3.48	3.43	3.08
	Standard deviation	0.09	0.11	0.29
CC′	1	4.12	3.82	4.22
	2	4.35	4.05	3.89
	3	4.48	4.74	3.91
	4	4.09	4.09	3.83
	5	4.29	4.21	3.83
	Average value	4.27	4.18	3.95
	Standard deviation	0.15	0.31	0.13
DD′	1	8.35	8.47	7.99
	2	9.01	8.12	7.91
	3	7.44	7.94	7.54
	4	7.36	8.12	7.85
	5	7.84	7.84	7.92
	Average value	7.99	8.09	7.85
	Standard deviation	0.68	0.23	0.17
AC	1	132.49	132.26	133.57
	2	132.61	132.76	133.14
	3	131.89	132.07	134.15
	4	132.20	131.62	133.90
	5	132.09	131.28	134.07
	Average value	132.26	131.99	133.77
	Standard deviation	0.29	0.55	0.38
BD	1	151.13	151.09	152.28
	2	151.08	151.12	152.29
	3	151.25	151.41	152.37
	4	151.19	151.22	152.54
	5	151.13	151.42	152.62
	Average value	151.16	151.25	151.42
	Standard deviation	0.04	0.15	0.15

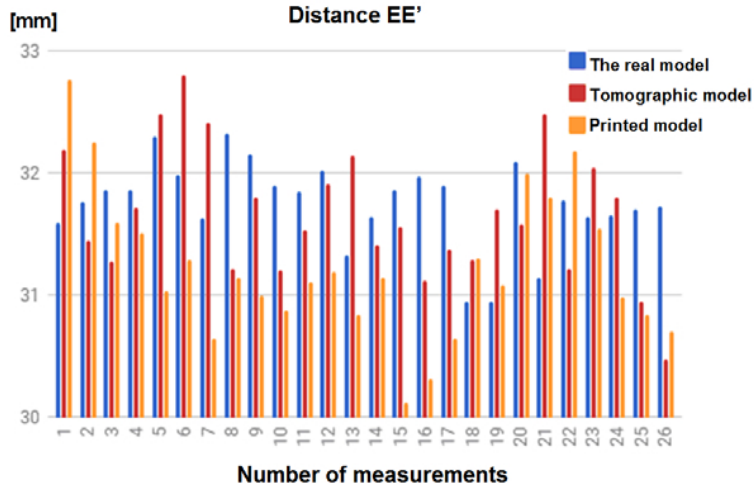

Fig. 10. Results for EE′ parameter measurements on a real model, tomography model and printed model

of skull bone structures depends considerably (approx. 12%) upon the software used and the precision of printer's kinematic systems [26, 27, 31].

Since the cranium constitutes a structure with complex sizes, for the selected cranial areas with variable curvature performed was an analysis of vectors of errors for the CT numerical model in relation to the reference model (Fig. 11) [31]. From the comparison of errors it may be concluded that their maximum value is 0.81 mm,

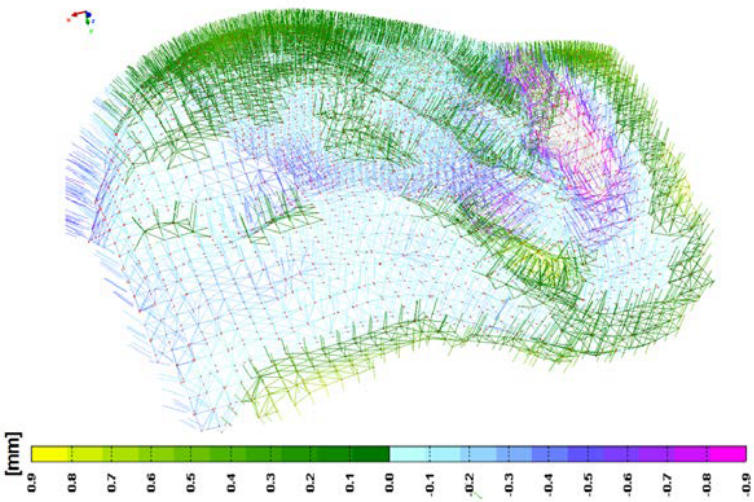

Fig. 11. Vectors of imaging precision errors for the cranium specimen from the zygomatic bone in the tomographic model vs., reference model

and the minimum is −0.98 mm. The standard deviation for the cranium specimen from the zygomatic bone amounted to 0.85 mm for 92% of measurements.

The problem of replication of bone structures of the skull and the accuracy of this mapping is a challenge for medical digital procedures, because it often determines the diagnosis and success of surgical treatment. In this type of reconstruction in clinical conditions, it is not possible to directly analyze the real object. For this purpose, it is advisable to carry out in vitro measurements taking into account the actual model and indication of errors that result from the measurement method and replication procedures. Based on the identification of real errors, you can have knowledge about their occurrence and location, as well as make error correction and optimization of measurements. At the same time it should be noted that the test object in the article – the skull – represents a serious challenge to metrology, due to the numerous outlines of a variable curvature.

4. Conclusions

The performed investigations allowed identifying the CT imaging precision for the skull bone structures, making a 3D model and replication of its shape in printed models.

An analysis of vectors of errors for the imaging of the shape of a selected cranial surface from the zygomatic bone enabled one to indicate the areas where CT imaging causes considerable errors resulting from the shape of the object under investigation.

While selecting a printing strategy in view of guaranteeing a proper precision of size and shape, of special importance is the assumption of correct procedures taking into consideration the division of the skull into components.

The completion of the investigations allows determining standard deviation in the procedures: CT imaging, making numerical models and printing 3D objects.

An evaluation of print imaging precision, based upon tomography models, may constitute a reliable tool in scheduling reconstruction operations on the skull, as well as in implantology and implant prosthetics.

Manuscript received by Editorial Board, June 18, 2018;
final version, December 19, 2018.

References

[1] D. Mitsouras, P. Liacouras, A. Imanzadeh, A.A. Giannopoulos, T. Cai, K.K. Kumamaru, and V.B. Ho. Medical 3D printing for the radiologist. *RadioGraphics*, 35(7):1965–1988, 2015. doi: 10.1148/rg.2015140320.

[2] F. Paulsen and J. Wasche. *Sobotta Atlas of Human Anatomy, General anatomy and musculoskeletal system*. Vol. 1, 2013.

[3] G.B. Kim, S. Lee, H. Kim, D.H. Yang, Y.H. Kim, Y.S. Kyung, and S.U. Kwon. Three-dimensional printing: basic principles and applications in medicine and radiology. *Korean Journal of Radiology*, 17(2):182–197, 2016. doi: 10.3348/kjr.2016.17.2.182.

[4] J.W. Choi and N. Kim. Clinical application of three-dimensional printing technology in craniofacial plastic surgery. *Archives of Plastic Surgery*, 42(3):267–277, 2015. doi: 10.5999/aps.2015.42.3.267.

[5] J.E. Loster, M.A. Osiewicz, M. Groch, W. Ryniewicz, and A. Wieczorek. The prevalence of TMD in Polish young adults. *Journal of Prosthodontics*, 26(4):284–288, 2017. doi: 10.1111/jopr.12414.

[6] A.S. Soliman, L. Burns, A. Owrangi, Y. Lee, W.Y. Song, G. Stanisz, and B.P. Chugh. A realistic phantom for validating MRI-based synthetic CT images of the human skull. *Medical Physics*, 44:4687–4694, 2017. doi: 10.1002/mp.12428.

[7] F. Heckel, S. Zidowitz, T. Neumuth, M. Tittmann, M. Pirlich, and M. Hofer. Influence of image quality on semi-automatic 3D reconstructions of the lateral skull base for cochlear implantation. *In CURAC*, 129–134, 2016.

[8] G. Budzik, T. Dziubek, and P. Turek. Basic factors affecting the quality of tomographic images. *Problems of Applied Sciences*, 3:77–84, 2015. (in Polish)

[9] S. Singare, C. Shenggui and N. Li. The Benefit of 3D Printing in Medical Field: Example Frontal Defect Reconstruction. *Journal of Material Sciences & Engineering*, 6(2):335, 2017. doi: 10.4172/2169-0022.1000335.

[10] A. Ryniewicz, K. Ostrowska, R. Knapik, W. Ryniewicz, M. Krawczyk, J. Sładek, and Ł. Bojko. Evaluation of mapping of selected geometrical parameters in computer tomography using standards. *Przegląd Elektrotechniczny*, 91(6):88–91, 2015. (in Polish) doi: 10.15199/48.2015.06.17.

[11] R. Kaye, T. Goldstein, D. Zeltsman, D.A. Grande, and L.P. Smith. Three dimensional printing: a review on the utility within medicine and otolaryngology. *International Journal of Pediatric Otorhinolaryngology*, 89:145-148, 2016. doi: 10.1016/j.ijporl.2016.08.007.

[12] G.T. Grant and P.C. Liacouras. Craniofacial Applications of 3D Printing. In: *3D Printing in Medicine: A Practical Guide for Medical Professionals*. Rybicki, Frank J., Grant, Gerald T. (Eds.), Springer, Cham, Switzerland, pp. 43–50, 2017. doi: 10.1007/978-3-319-61924-8_5.

[13] T. Cai, F.J. Rybicki, A.A. Giannopoulos, K. Schultz, K.K. Kumamaru, P. Liacouras, and D. Mitsouras. The residual STL volume as a metric to evaluate accuracy and reproducibility of anatomic models for 3D printing: application in the validation of 3D-printable models of maxillofacial bone from reduced radiation dose CT images. *3D Printing in Medicine*, 1(1):2, 2015. doi: 10.1186/s41205-015-0003-3.

[14] T.Y. Hsieh, B. Cervenka, R. Dedhia, E.B. Strong, and T. Steele. Assessment of a patient-specific, 3-dimensionally printed endoscopic sinus and skull base surgical model. *JAMA Otolaryngology–Head & Neck Surgery*, 144(7):574-579, 2018. doi: 10.1001/jamaoto.2018.0473.

[15] Y.W. Chen, C.T. Shih, C.Y. Cheng, and Y.C. Lin. The development of skull prosthesis through active contour model. *Journal of Medical Systems*, 41:164, 2017. doi: 10.1007/s10916-017-0808-2.

[16] J.S. Naftulin, E.Y. Kimchi, and S.S. Cash. Streamlined, inexpensive 3D printing of the brain and skull. *PLoS One*, 10(8):e0136198, 2015. doi: 10.1371/journal.pone.0136198.

[17] A. Ryniewicz, K. Ostrowska, Ł. Bojko, and J. Sładek. Application of non-contact measurement methods for the evaluation of mapping the shape of solids of revolution. *Przegląd Eletrotechniczny*, 91(5):21–24, 2015. (in Polish). doi: 10.15199/48.2015.05.06.

[18] V. Favier, N. Zemiti, O.C. Mora, G. Subsol, G. Captier, R. Lebrun. and B. Gilles. Geometric and mechanical evaluation of 3D-printing materials for skull base anatomical education and endoscopic surgery simulation – A first step to create reliable customized simulators. *PloS One*, 12(12): e0189486, 2017. doi: 10.1371/journal.pone.0189486.

[19] M.P. Chae, W.M. Rozen, P.G. McMenamin, M.W. Findlay, R.T. Spychal, and D.J. Hunter-Smith. Emerging applications of bedside 3D printing in plastic surgery. *Frontiers in Surgery*, 2:25, 2015. doi: 10.3389/fsurg.2015.00025.

[20] J.A. Sładek. *Coordinate Metrology. Accuracy of Systems and Measurements*. Springer, 2015.
[21] ISO 15530-3:2011: Geometrical product specifications (GPS) – Coordinate measuring machines (CMM): Technique for determining the uncertainty of measurement – Part 3: Use of calibrated workpieces or measurement standards.
[22] A. Marro, T. Bandukwala, and W. Mak. Three-dimensional printing and medical imaging: a review of the methods and applications. *Current Problems in Diagnostic Radiology*, 45(1): 2–9, 2016. doi: 10.1067/j.cpradiol.2015.07.009.
[23] A. Ryniewicz. *Evaluation of the accuracy of the surface shape mapping of elements of biobearings in in vivo and in vitro tests*. Scientific Works of the Warsaw University of Technology. Mechanics, 248:3–169, 2013. (in Polish).
[24] B.M. Mendez, M.V. Chiodo, and P.A. Patel. Customized "In-Office" three-dimensional printing for virtual surgical planning in craniofacial surgery. *The Journal of Craniofacial Surgery*, 26(5):1584–1586, 2015. doi: 10.1097/SCS.0000000000001768.
[25] J.J. de Lima Moreno, G.S. Liedke, R. Soler, H.E.D. da Silveira, and H.L.D. da Silveira. Imaging factors impacting on accuracy and radiation dose in 3D printing. *Journal of Maxillofacial and Oral Surgery*, 17(4):582–587, 2018. doi: 10.1007/s12663-018-1098-z.
[26] S.W. Park, J.W. Choi, K.S. Koh and T.S. Oh. Mirror-imaged rapid prototype skull model and pre-molded synthetic scaffold to achieve optimal orbital cavity reconstruction. *Journal of Oral and Maxillofacial Surgery*, 73(8):1540–1553, 2015. doi: 10.1016/j.joms.2015.03.025.
[27] K.M. Day, P.M. Phillips, and L.A. Sargent. Correction of a posttraumatic orbital deformity using three-dimensional modeling, Virtual surgical planning with computer-assisted design, and three-dimensional printing of custom implants. *Craniomaxillofacial Trauma and Reconstruction*, 11(01):078–082, 2018. doi: 10.1055/s-0037-1601432.
[28] Y.C. Lin, C.Y. Cheng, Y.W. Cheng, and C.T. Shih. Skull repair using active contour models. *Procedia Manufacturing*, 11: 2164–2169, 2017. doi: 10.1016/j.promfg.2017.07.362.
[29] J.N. Winer, F.J. Verstraete, D.D. Cissell, S. Lucero, K.A. Athanasiou and B. Arzi. The application of 3-dimensional printing for preoperative planning in oral and maxillofacial surgery in dogs and cats. *Veterinary Surgery*, 46(7):942–951, 2017. doi: 10.1111/vsu.12683.
[30] J.Y. Lim, N. Kim, J.C. Park, S.K. Yoo, D.A. Shin, and K.W. Shim. Exploring for the optimal structural design for the 3D-printing technology for cranial reconstruction: a biomechanical and histological study comparison of solid vs. porous structure. *Child's Nervous System*, 33(9):1553–1562, 2017. doi: 10.1007/s00381-017-3486-y.
[31] W. Shui, M. Zhou, S. Chen, Z. Pan, Q. Deng, Y. Yao, H. Pan, T. He, and X. Wang. The production of digital and printed resources from multiple modalities using visualization and three-dimensional printing techniques. *International Journal of Computer Assisted Radiology and Surgery*, 12(1):13–23, 2017. doi: 10.1007/s11548-016-1461-9.